

DETERMINATION OF ELASTIC PROPERTIES BY AN ULTRASONIC TECHNIQUE

S. Baste

*Université Bordeaux 1, Laboratoire de Mécanique Physique, CNRS UPRES A 5469
351, Cours de la Libération, 33405-TALENCE Cedex, France*

SUMMARY: The main purpose of this paper is to show the reliability and the accuracy of ultrasonic elastic behaviour characterisation. Firstly, the main principles of ultrasonic NDE, i.e., an inverse problem which involves an optimal recovery of the complete stiffness matrix from time of flight measurements, is briefly reviewed. The numerical processing of the wave velocities data, which enables the identification of all the stiffness coefficients of an orthorhombic material, is described. The reliability and accuracy of the identification are discussed.

KEYWORDS: Ultrasonic - Characterisation -Anisotropy.

INTRODUCTION

Because of their texture, composite materials are strongly anisotropic. Measurement of the nine elastic constants constituting the stiffness matrix by the classical static technique - loading and extensometry - requires a large number of samples with suitable orientations. However, such sample cuts are often unavailable from the manufacturing process and a full evaluation cannot be achieved this way. Ultrasonic bulk waves NDE appears nowadays as one of the best approaches in experimental solid mechanics. But as ultrasonic values are related to the stiffness constants, comparison between the two methods involves a matrix inversion. So, because such a full comparison is not always possible, mechanical engineers had a little confidence in ultrasonic results.

The determination of the elastic properties of elastic anisotropic solids has been tackled first by using measurements of ultrasonic phase velocity along predetermined directions of high symmetry. Simple expressions relate particular elasticity constants, or combinations thereof, to individual velocities [1-3]. However, these ultrasonic contact methods that require as well cutting the sample in various directions to allow access to all constants, are sensitive to the error propagation in calculations. Transmission of bulk waves through materials immersed in water is better appropriated to measure the stiffness tensor [4,5]. By using mode conversion at a liquid-solid interface, one quasi longitudinal and two quasi transverse bulk waves can be generated and transmitted in numerous directions in the solid [6]. The phase velocities of bulk waves in the medium are related to the elasticity constants of an anisotropic medium through

the well-known Christopher equation [6]. By inverting this equation, the elasticity constants can be determined from a suitable set of experimental velocities for various directions.

The main difficulty is related to the convergence of the inversion algorithm. Clearly the difficulties of convergence decrease as the number of unknowns decreases. This explains that the orthorhombic symmetry is considered as general enough to describe the anisotropy of most of composite materials. This class of symmetry is indeed characterised by nine independent moduli if the coincidence between the symmetry axes and the geometric axes of the sample is assumed. However, difficulties of convergence remain when simultaneous determination of the nine stiffnesses is carried out. The problem of nine unknowns is then reduced to one direct calculation followed by two problems of three unknowns and then by a problem of two unknowns [7]. These three minimisations do not pose any difficulty of convergence and classically identify the nine moduli of a material that presents a symmetry greater than orthorhombic symmetry, for example tetragonal or isotropic symmetry.

Questions still remain regarding the suitability of this method for elastic property characterisation. Of particular concern is the sensitivity of experimental measurements to all moduli and, since one is dealing with a system of non-linear equations, error propagation in calculations. A possibility is to recognise *a posteriori*, from variances and covariances delivered by the optimisation procedure, which stiffnesses have been most accurately recovered and which lessso.

The establishing of the ultrasonic characterisation reliability requires the full characterisation of a composite for which, because of its very good homogeneity at the frequencies used, the accuracy enables the matrix inversion. The inversion of identified stiffness coefficients gives the value of the Young modulus in the fibre direction. It is to be compared with the measurements realised on the same sample by extensometric tensile test.

ULTRASONIC CHARACTERISATION

In anisotropic solid exhibiting a purely elastic behaviour, the stress-strain relationship is:

$$\sigma_{ij} = C_{ijkl} \epsilon_{kl} , \quad (1)$$

Substituting a small displacement field of anelastic plane bulk wave [6] :

$$U(\mathbf{X}, t) = a \cdot \mathbf{P} \exp. ik(\mathbf{n} \cdot \mathbf{X} - Vt) \quad (2)$$

where the displacement field \mathbf{U} at any point \mathbf{X} at the time t appears to be a plane wave with an amplitude a , the polarisation vector \mathbf{P} , travelling in the direction \mathbf{n} with the phase velocity V , and where the frequency f and the wave number k are related through the dispersion equation $k = 2\pi f/v$, into the equation of motion leads to the wave equation written under the Christoffel form:

$$\left(\Gamma_{ij} - \rho V^2 \delta_{ij} \right) P_j = 0, \quad (3)$$

with $\Gamma_{ij} = C_{ijkl} n_k n_l$, $i, j, k, l = 1, 2, 3$ and where ρ is the density. Since the operator Γ_{ij} is symmetric, its eigenvalues ρV^2 are real and the respective eigenvectors \mathbf{P} are mutually orthogonal. So, three modes can propagate along the direction \mathbf{n} with three different velocities and their associated polarisation vectors. For special propagation directions such as the material principal directions, they are reduced to pure modes: longitudinal when $\mathbf{P} = \mathbf{n}$ or transverse when $\mathbf{P} \cdot \mathbf{n} = 0$. In the general case, modes are not pure: one quasi longitudinal (QL), a fast (QT1) and a slow (QT2) quasi transverse waves are excited. Their velocities are the solution of the following third-degree equation in the unknown ρV^2 :

$$\det \left(\Gamma_{ij} - \rho V^2 \delta_{ij} \right) = 0. \quad (4)$$

If the phase velocities for a given propagation direction \mathbf{n} are known, the stiffnesses (C_{ijkl}) are obtained by inverting Eq. (4). Every measured wave speed V_p is approximately the solution of the non-linear cubic equation, expanded form of the Christoffel equation. Due to the experimental errors, the following function is close to zero:

$$f_p(C_{IJ}, \lambda_p, \mathbf{n}) = -\lambda_p^3 + \lambda_p^2(\Gamma_{11} + \Gamma_{22} + \Gamma_{33}) + \lambda_p(\Gamma_{12}^2 + \Gamma_{13}^2 + \Gamma_{23}^2 - \Gamma_{11}\Gamma_{22} - \Gamma_{11}\Gamma_{33} - \Gamma_{22}\Gamma_{33}) + \Gamma_{11}\Gamma_{22}\Gamma_{33} + 2\Gamma_{12}\Gamma_{23}\Gamma_{13} - \Gamma_{11}\Gamma_{23}^2 - \Gamma_{22}\Gamma_{13}^2 - \Gamma_{33}\Gamma_{12}^2 \approx 0, \quad (5)$$

where $\lambda_p = \rho V_p^2$ and $p=1$ to N , N is the total number of measurements. Identification of the elasticity constants from wave speed measurements in various propagation directions is performed by minimising the functional:

$$F(C_{IJ}) = \sum_{p=1}^N \{f_p(C_{IJ}, \lambda_p, \mathbf{n})\}^2 \quad (6)$$

build from the overdetermined system of equations(5). N is generally greater than the number of unknowns.

Recovering the full set of the components of the stiffness tensor is an inverse problem of the secular equation (4). Elasticity constants have to be recovered as the coefficients of the secular equation from suitable sets of experimental values of its roots ρV^2 in various directions \mathbf{n} . It is quite a classical problem in numerical analysis which is solved by an optimisation algorithm under some constraints of a non-linear functional in the sense of the least squares [5, 6].

ACQUISITION OF ULTRASONIC WAVES

Wavespeed measurements are performed by using ultrasonic pulses which are retransmitted through a plate immersed in water, Fig. 1. Ultrasound was generated and sensed by a pair of piezoelectric transducers supported by goniometers which allow one to select any propagation direction \mathbf{n}_i of incident wave. The coordinate system $R=(\mathbf{x}_1, \mathbf{x}_2, \mathbf{x}_3)$ for ultrasonic measurements is chosen in such a way that axis \mathbf{x}_1 corresponds to the normal to the interface.

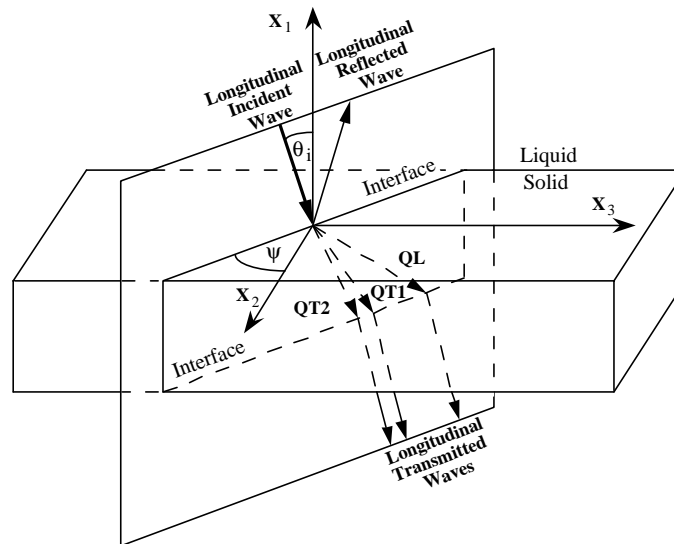


Fig. 1: Simple-transmission experiment. The incident plane is defined by the azimuthal angle ψ .

For an oblique incident angle, the longitudinal incident pulse is refracted at the liquid-solid interface and generates one, two or three waves that propagate with different velocities along the directions $\mathbf{n}=\mathbf{n}_m$, $m=1, 2$ or 3 . So 1, 2 or 3 modes reach the receiver with time delay depending on their respective velocities. Continuity of displacements and constraints at the

interface gives the number of waves effectively generated in the solid. The incident wave in water is obviously a pressure wave. With such an incident wave, the Snell laws of refraction show that only the two QL and QT2 modes are generated if the incident plane coincides with a plane of symmetry. In this case, the third wave of pure transverse character has a particle displacement parallel to the surface of the sample and cannot be generated [6]. Furthermore, whatever the plane of incidence, the wavespeed in water is usually less than any mode wavespeed in the solid. So, limit angles of incidence occur for which the refracted wave in the solid becomes evanescent and does not reach the receiver. Consequently, wavespeed data are angular areas inside which the transmitted amplitudes through the two interfaces, as shown in figure 2, have an appropriated signal /noise ratio.

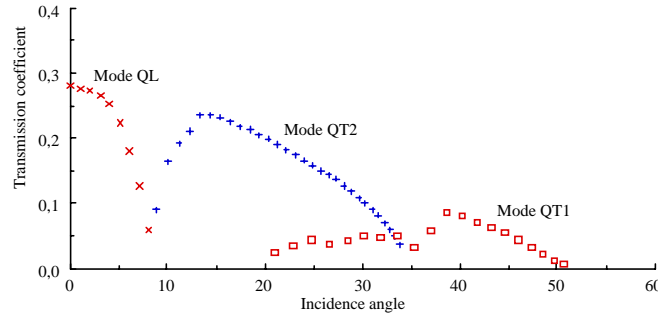


Fig.2: Transmission coefficients for the three modes in a $\Psi = 45^\circ$ plane versus incidence angle.

Choice of the frequency

Most composite materials contain voids, pores or micro-cracks in relation to their manufacturing process and texture. As long as their size and the texture scales are small compared to the wavelength, the wave attenuation is an anisotropic diffusion process. In the low frequency range, the medium will act as a low-pass filter decaying with a parabolic profile. Its cut-off frequency is in close relation [8] with the scatterers' effective area and their concentration.

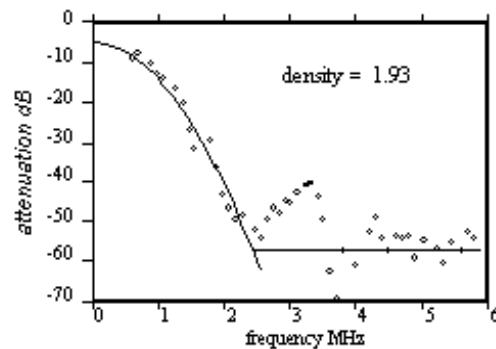


Fig. 3: Transfer function at normal incidence of a 2D C-SiC composite material.

At higher frequencies, as shown on figure 3, resonances and anti-resonances appear in connection with the structural scales. The transition frequency and the exponent in the parabolic part are well related to the porosity and the mean size of the voids [9, 10]. Of course, above this frequency, the medium may no longer be assumed homogeneous and the Christoffel's equation does not apply.

Successful application of the method depends critically on an appropriate selection of the central frequency. Frequency has to be sufficiently low for the measurement to be representative of the elementary volume response but at the same time high enough to achieve a separation between the QL and the QT waves.

The limitations to the application range of this technique are essentially of dimensional order. The wave length of the generated wave shall be short enough for the assumption of a semi-infinite body to be met. The spectral range is limited for the high frequencies (i. e. the short wave lengths) by a strong absorption and by the fact that the requirement of homogeneity with regard to structural scale of the material is not respected. The experimental frequency-range being sometime very narrow, temporal overlapping of signals becomes important and the echoes which are in the multi-mode reflected pulse, cannot be easily separated.

The central frequency will have an upper limit value : $f \ll V/d$ where d is a characteristic dimension for example the thickness of a layer, and a lower limit value : $f > 3 V / 2 e$ where e is the thickness of the sample; this lower limit will depend on the time duration of the impulsive response and will allow the separation of multiple echoes which overlap because of : internal reflections, mixing of modes or scattering.

The temporal and spectral waveforms are sometimes quite different that a homogeneous plate's ones, see for example the one of a 3D EvoC/C at 2,25 MHz frequency (Fig. 4). We can see the generation of two modes at normal incidence.

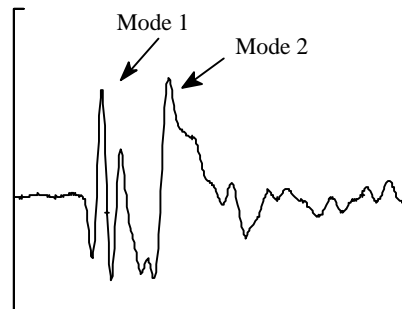


Fig. 4: .Temporal waveform at 2,25 MHz of a 3D Evo C/C.

Assumption of homogeneous material, associated with propagation of bulk waves, is available under a high cut-off frequency near to 5 MHz. The generation, below the high cut-off frequency, of a guided mode of which the low cut-off frequency is between 1 MHz and 2 MHz, justifies the simultaneous presence of two waves in the temporal waveform of the 3D Evo C/C at 2.25 MHz or 5 MHz frequencies. The existence of an optical mode (guided mode) at low frequencies, below the high cut-off frequency of the acoustical mode, is often detected in 3D C/C composite [11]. The mode 2 corresponding to a bulk wave is the only one generated below the low cut-off frequency of the guided mode. The high value of the cut-off frequency of the bulk waves (> 5 MHz) and of the low cut-off frequency of the guided mode (> 1 MHz) allow an elastic evaluation of the 3D Evo C/C by immersion interferometer.

phase velocity measurements

An appropriate signal processing of the received pulses is performed by using a reference signal propagating in water without the sample [4]. The time-of-flight difference [4] between reference (through fluid) and through the sample (at incident angle θ_i) acoustic paths is given by:

$$\delta t = \frac{e}{V_0} \left(\cos \theta_i - \sqrt{\left(\frac{V_0}{V} \right)^2 - \sin^2 \theta_i} \right), \quad (7)$$

where V_0 is the sound speed in water and V is the phase velocity in the sample, θ_i is the incident angle. As demonstrated for this experimental device [12], the time delay caused by the presence of the anisotropic plate is equal to the time for an acoustic wave propagating with the phase velocity inside the material. The phase velocity in the sample is then determined from the time-of-flight difference δt measurement:

$$V = \frac{V_0}{\sqrt{1 + \frac{V_0}{e} \delta t \left(\frac{V_0}{e} \delta t - 2 \cos \theta_i \right)}}. \quad (8)$$

When the thickness of the plate is comparatively too small to the wavelength or when scattering due to the material inhomogeneities is too large, signal processings become inaccurate and even ineffective. Waves overlapping due to multiple reflections or mode conversion at interface donot allow the spatial or temporal separation of different modes. Identification of the stiffness tensor suffers from inaccuracy of time-delay measurements caused by mode mixing. The success of the (C_{IJ}) determination rests on the ability of the signal processing to improve the time resolution of overlapped waves when dispersive effects are present[13]. The choice of the central frequency of transducers according to the characteristic length of the material is crucial.

Among the signal processings used for the time-delay δt measurements, the location of the vertical asymptote of the Hilbert transform is from many points of view the most appropriate to the non destructive evaluation of the elasticity constants [13]. The best resolution of overlapped waves enables one to decrease the smallest measured value of the temporal shift between the modes, and consequently to decrease the central frequency of the transducers chosen in regard to the scattering effects. This signal processing measures phase velocity corresponding to the lowest frequencies included in the signal bandwidth. This unambiguous measurement of phase velocity leads to the determination of the stiffnesses independently from the attenuation mechanisms. On the contrary, when dispersion is significant ,cross-correlation processing gives values that one can link neither to group velocity nor to phase velocity [13] without additional assumptions on attenuation mechanisms.

Using the Hilbert transform the velocity at normal incidence ($\theta_i=0_j$) is measured from the time-of-flight difference $\delta t'$ between the through-sample and the fluid paths. The time delay δt of a wave at arbitrary oblique incidence (θ_i-0_j) is: $\delta t = \delta t^* + \delta t'$, where δt^* is the time delay, obtained by the Hilbert transform, between this signal and the signal at normal incidence. Taking the transmitted signal at normal incidence as reference [12, 13] improves the accuracy of the δt measurement. The advantage of such a method is especially important when dispersion effects are present. The shapes of the transmitted signals to be compared are closer.

Phase velocities V_p at incident angle θ_i , imposed by the goniometers, are collected in several incident planes (\mathbf{x}_1, Ψ) , where Ψ is the azimuthal angle (Fig. 1). The number of these experimental data is always greater than the number of elasticity constants to be identified. Since the refraction angles $\theta_r = (\mathbf{x}_1, \mathbf{n}_m)$, $m=1, 2$ or 3 , of the phase velocities are directly related to the angle of incidence through Snell-Descartes' laws, calculation of V_p from Eq. (8) allows the building of the system (6).

RECOVERING OF THE STIFFNESS TENSOR.

The maximum number of independent elasticity constants is twenty-one for any medium. Usually this number is less because of additional restrictions imposed by the symmetry of the medium. The orthorhombic symmetry is considered as general enough to describe the anisotropy of most of composite materials. Respectfully this assumption on the material symmetry that imply existence of three mutually orthogonal planes of symmetry, if the knowledge of the material symmetry axes and the coincidence between the symmetry axes and the geometric axes of the sample are assumed, and using the abbreviated subscripts notation, the elasticity tensor (C_{IJ}) is expressed by the nine non-zero components of a symmetric (6 x 6) matrix:

$$(C_{IJ}) = \begin{pmatrix} C_{11} & C_{12} & C_{13} & 0 & 0 & 0 \\ & C_{22} & C_{23} & 0 & 0 & 0 \\ & & C_{33} & 0 & 0 & 0 \\ & & & C_{44} & 0 & 0 \\ & \text{Sym.} & & & C_{55} & 0 \\ & & & & & C_{66} \end{pmatrix} \quad (9)$$

According to the degree of material anisotropy, the number of unknowns that is the number of independent elasticity constants, varies from two to nine for the isotropic to the orthorhombic symmetry.

Simultaneous determination of the nine moduli from Eq.(6) and from the set of experimental velocities measured in the planes $(\mathbf{x}_1, \mathbf{x}_2)$, $(\mathbf{x}_1, \mathbf{x}_3)$ and $(\mathbf{x}_1, \mathbf{45}_j)$ can be performed [14]. But,

the domain of convergence is sometimes too narrow. To improve the convergence of the inversion algorithm, the stiffness tensor is identified by several steps. The planes of wave speed measurements are treated separately.

The stiffness C_{11} is determined directly from the phase velocity measured at normal incidence. C_{22} , C_{12} , C_{66} and C_{33} , C_{13} , C_{55} are respectively identified from velocity measurements in the two accessible planes of symmetry $(\mathbf{x}_1, \mathbf{x}_2)$ and $(\mathbf{x}_1, \mathbf{x}_3)$. The last step processes the data collected in the non symmetry plane $(\mathbf{x}_1, \mathbf{45}_i)$ for which Eq. (5) does not factorize. The unknowns are reduced to the two remaining constants C_{44} and C_{23} and the previous seven values of stiffnesses are used as data. The inverse problem is reduced to three distinct minimisations of the factorised or non-factorised Christoffel equation. These minimisations present no difficulty of convergence and identify the nine elasticity constants of a material with a symmetry higher than orthorhombic symmetry.

When dealing with the propagation in one of these three planes of symmetry, Eq. (5) factorizes, for example in the plane $(\mathbf{x}_1, \mathbf{x}_2)$:

$$f_p(C_{IJ}, \lambda_p, \mathbf{n}) = (\Gamma_{33} - \lambda_p) (\lambda_p^2 - \lambda_p(\Gamma_{11} + \Gamma_{22}) + \Gamma_{11}\Gamma_{22} - \Gamma_{12}^2), \quad (10)$$

where the trivial eigenvalue $\lambda_p (= \Gamma_{33})$ corresponds to a pure transverse mode polarised along the direction \mathbf{x}_3 . This wave cannot be generated from fluid in the plane $(\mathbf{x}_1, \mathbf{x}_2)$. The subscript QT denotes the quasi transverse mode that can be excited in the sample and measured. For the plane $(\mathbf{x}_1, \mathbf{x}_2)$, Eq. (5) is reduced to a quadratic equation:

$$f_p^{(12)}(C_{IJ}, \lambda_p, \mathbf{n}) = (\lambda_p^2 - \lambda_p(\Gamma_{11} + \Gamma_{22}) + \Gamma_{11}\Gamma_{22} - \Gamma_{12}^2), \quad (11)$$

and then, introduced in the Euclidean functional(6). When the thickness of the sample does not allow one to collect data in the principal plane $(\mathbf{x}_2, \mathbf{x}_3)$, only a partial set of elasticity constants can be determined from ultrasonic measurements in the planes $(\mathbf{x}_1, \mathbf{x}_2)$ and $(\mathbf{x}_1, \mathbf{x}_3)$. Therefore, a third plane, for example the plane $(\mathbf{x}_1, \mathbf{45}_i)$, is introduced in the identification process[7].

The optimum values of the stiffness coefficients, in the least square sense, are those for which the non-linear function (4) reaches its minimum value for the whole set of experimental data.

RELIABILITY AND ACCURACY

Questions still remain regarding the suitability of this method for elastic property characterization. Of particular concern is the sensitivity of experimental measurements to all moduli and, since one is dealing with a system of non-linear equations, error propagation in calculations. The accuracy of reconstruction may been investigated by several approaches. For example, the sensitivity coefficients, i.e., the dependence of phase velocity on elasticity constants is estimated numerically [15], analytically by a perturbation method [16], or pragmatically by analyzing [17] the effects of the initial guesses, experimental data random scatter and the range of the refraction angle. Another possibility is to recognise *a posteriori*, from variances and covariances delivered by the optimisation procedure, which stiffnesses have been most accurately recovered and which less so. It amounts to estimating a confidence interval associated with each identified constant can be calculated [18] by means of a statistical analysis of the set of velocity measurements in each incident plane. The values $I_{90\%}(C_{IJ})$ are deduced from a linearisation of Eq. (5) around the exact solution for each measured velocity. Since some assumptions on the angular distribution of the deviation between the measured and there calculated velocities are required, that does not provide an exact calculation. Nevertheless, since these confidence intervals are sensitive[18] to the level of experimental data scatter and to the angle range of these velocity data, that enables one to

establish the reliability of ultrasonic characterization. That quantifies the sensitivity of the inversion algorithm for identifying elasticity constants from wave speed data.

The establishing of the ultrasonic characterisation reliability requires the comparison of its identification with classical mechanical measurements of Young modulus. But, the ultrasonic values being related to the stiffness constants, comparison between the two methods involves a matrix inversion. For this purpose, we have completely characterized an unidirectional Carbon-Epoxy sample for which, because of its very good homogeneity at the frequencies used, the accuracy enables the matrix inversion. The stiffness coefficients identified, and their relative 90 % confidence interval are reported below (GPa):

$$C = \begin{pmatrix} 12.35 & 5.47 & 5.44 & & & \\ & 12.54 & 7.24 & & & \\ & & 135.8 & & & \\ & & & 6.9 & & \\ & \text{sym.} & & & 6.20 & \\ & & & & & 3.53 \end{pmatrix} \pm \begin{pmatrix} 0.04 & 0.07 & 0.25 & & & \\ & 0.09 & 0.27 & & & \\ & & 3.9 & & & \\ & & & 0.359 & & \\ \text{sym.} & & & & 0.10 & \\ & & & & & 0.06 \end{pmatrix}_{90\%} \quad (12)$$

The solid line curves are drawn from these constants and the secular equation (4). The good fit with the experimental data is a consequence of the very good homogeneity of this material and its fine texture. Furthermore, in the (1,2) plane, which is not displayed here, the anisotropy factor : $2C_{66} / (C_{22} - C_{12})$ is close to one and this plane may be considered as isotropic. So, for such a material, with long fibres along the axis 3, a hexagonal texture described by only 5 independent constants would be sufficient. However we found that C_{11} and C_{22} differ by more than 5 times their confidence interval and the same for C_{13} and C_{23} . One can say therefore that the expected six fold symmetry around the 3axis is a coarse approximation.

The inversion then gives the value of the Young modulus in the direction 3: $E_3 = 131 \pm 5$ GPa. It is to be compared with the measurements realised on the same sample by repetition of numerous extensometric tensile tests which give values comprised between 130 and 150 GPa.

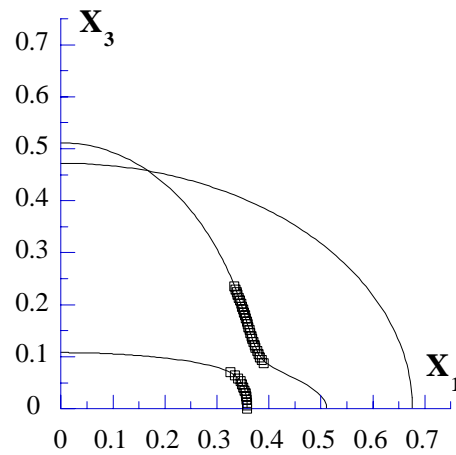
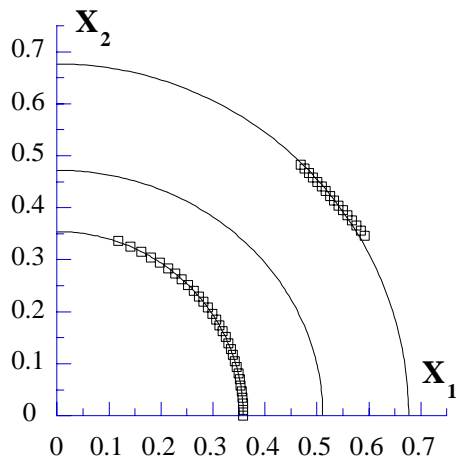
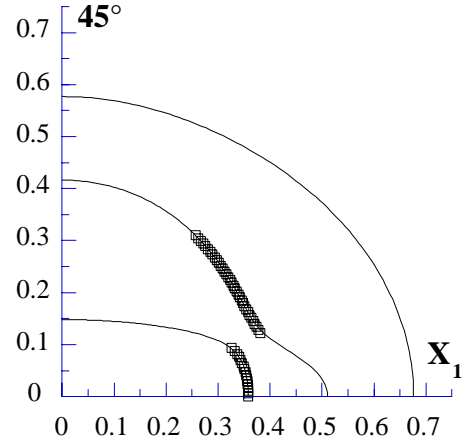


Fig. 5: Slownesses ($\mu\text{s}/\text{mm}$) for a 1D carbon-epoxy in the $(\mathbf{x}_1, \mathbf{x}_2)$, $(\mathbf{x}_1, \mathbf{x}_3)$ and $(\mathbf{x}_1, 45^\circ)$ planes. The points are experimentally measured slownesses. The solid lines are slownesses calculated from the reconstructed elasticity constants.



More spread data as shown on figure 6 are observed for a ceramic-ceramic SiC-SiC composite with a coarse texture and an important porosity (around 20% in volume). Of course, confidence intervals become larger. In such a sample only 3 mm thick along axis 1 and a 0.5 mm periodicity along axis 2 and 3, we are close to the limits of the scales of homogeneity. Then, the ultrasonic wave velocity measurement is of less quality and it leads to a more extended confidence interval associated to the identified constants.

For this SiC-SiC 2D sample, the stiffness matrix, and its 90 % confidence interval are in GPa:

$$C = \begin{pmatrix} 169 & 48.3 & 50.3 & 0 \\ & 297 & 148 & 0 \\ & & 331 & 75 \\ & \text{sym.} & & 58.8 \\ & & & & 57.8 \end{pmatrix} \pm \begin{pmatrix} 2 & 3.3 & 3.8 & 0 \\ & 13 & 42 & 0 \\ & & 16 & 23 \\ & \text{sym.} & & 1.0 \\ & & & & 1.0 \end{pmatrix} \quad (13)$$

Pulses of QL and QT2 waves are time overlapped because the strong scattering of the waves acts as a low-pass filter spreading the pulse durations. Such a material illustrates the present limits of this technology. However inaccurate results are preferable to no results, unavailable by other means.

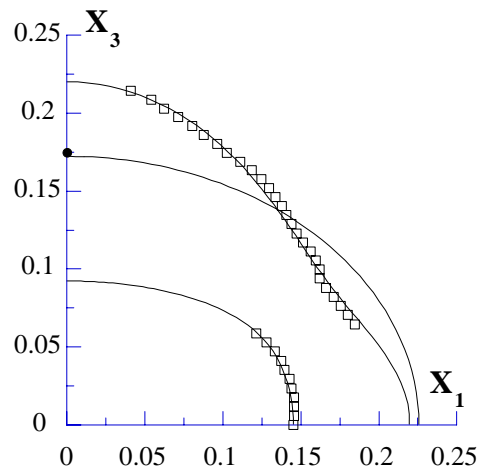
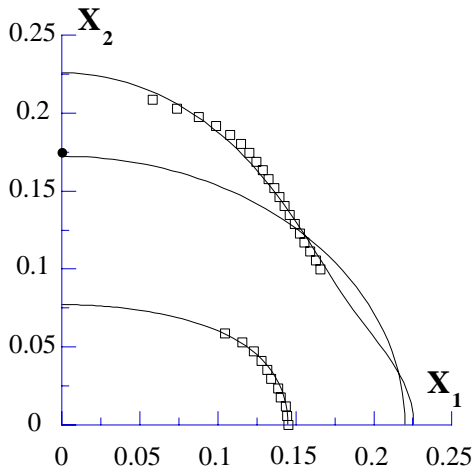
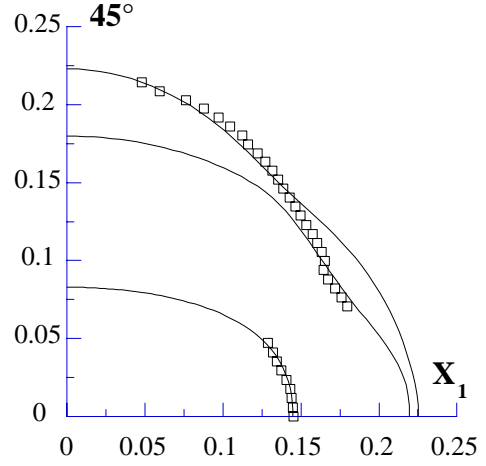


Fig. 6: Slownesses ($\mu\text{s}/\text{mm}$) for a 2DSiC-SiC composite in the $(\mathbf{x}_1, \mathbf{x}_2)$, $(\mathbf{x}_1, \mathbf{x}_3)$ and $(\mathbf{x}_1, 45^\circ)$ planes. The points are experimentally measured slownesses. The solid lines are slownesses calculated from the reconstructed elasticity constants.



Accuracy improvements in the stiffness matrix recovery are a function of two parameters: the angular range of data and the accuracy of each wave speed value. It has been demonstrated [17] that the latter is the main factor since the angular aperture is only stated by the refraction laws, i.e., the wave speed ratios between water and solid. Comparison between figures 5 and 6 illustrates the fact that a small amount of accurate data in a narrow range is more suitable than imprecise data obtained on a wider angular range.

CONCLUSION

Ultrasonic NDE of various anisotropic elastic media by bulk waves appears nowadays as one of the best approaches in experimental solid mechanics. It is also the only way to study composite materials that cannot be manufactured in any other shape than laminate plates and for which sample cuts in various directions are not available. Measurements under load also enable considerable progress to be made in theory and assessments of damage and fracture mechanisms.

However, to avoid errors and spurious results, the limitations of the method must be always kept in mind. Samples must be homogeneous at all structural scales neither too thin nor too porous. Bulk wave propagation would not be correctly described by plane waves propagating in a virtually free homogeneous space.

Furthermore, water immersion technology is, of course, limited to ambient temperatures. Today, improvements are reported in experiments using air propagation [19] and non-contact devices with laser generation and reception [20] more appropriated to high temperature investigations.

REFERENCES

1. Neighbours J. R. and Schacher G. E., «Determination of elastic constants from sound-velocity measurements in crystals of general symmetry,» J. Appl. Phys. 38,1967, pp. 5366-5375.
2. Van Buskirk W. C., Cowin S. C. and Carter Jr R., «A theory of acoustic measurement of the elastic constants of a general anisotropic solid,» J. Mat. Sci. 21, 1986, pp.2749-2762.
3. Norris A. N., «On the acoustic determination of the elastic moduli of anisotropic solids and acoustic conditions for the existence of symmetry planes,» Q. J. Mech. Appl. Math. 42, 1989, pp. 412-426.
4. Roux J., Hosten B., Castagnède B. and Deschamps M., "Caractérisation mécanique des solides par spectro-interférométrie ultrasonore". Rev. Phys. Appl.20, 1985, pp. 351-358.
5. Castagnède B., Jenkins J.T., Sachse W. and Baste S., "Optimal determination of the elastic constants of composite materials from ultrasonic wave speed measurements". J.Appl.Physics, 67, 6, 1990, pp. 2753-2761.
6. Auld B.A. "AcousticFields and Waves in Solids", Wiley Interscience; N. Y., 1973.
7. Baste S. and Hosten B., "Evaluation de la matrice d'élasticité des composites orthotropes par propagation ultrasonore en dehors des plans principaux de symétrie", Rev. Phys. App. 25, 1990, pp. 161-168 .
8. Truell R., Elbaum C.and Chick B.B. " Ultrasonic Methods in Solid State Physics". Acad. PressN.Y., 162, 1969.
9. Tittmann B.R., HostenB. and Abdel-Gawwad M., " Ultrasonic attenuation in Carbon-Carboncomposites and the determination of porosity ". Proceed. IEEE Ultrasonics Symp. Williamsburg, 1986.
10. Gubernatis J.E. and Domany E. "Effects of Microstructure on the Speed and Attenuation of Elastic Waves". Rev.of Progress in QNDE, 3B,1984, pp. 1129-1135.
11. Baste S. and Gerard A., "Etude des modes guidés dans les composites tri-directionnels". Revue d'Acoustique, n°78, 1986.
12. Rokhlin S. I. and Wang W., «Double through-transmission bulk wave method for ultrasonic phase velocity measurement and determination of elastic constants of composite materials,» J. Acoust. Soc. Am. 91, 1992, pp.3303-3312 .
13. Audoin B. and Roux J., «A innovative application of the Hilbert transform to time delay estimation of overlapped ultrasonic echoes,» Ultrasonics 34, 1996, pp.25-33.
14. Aristégui Ch. and Baste S., "Optimal recovery of the elasticity tensor of general anisotropic materials from ultrasonic velocity data", J. Acoust.Soc. Am., Vol. 101, n°2, 1997, pp. 813-833.
15. Kline R. A. and Sahay S. K., «Sensitivity analysis for elastic property reconstruction of anisotropic media,» in Review of Progress in Quantitative Non destructive Evaluation, Plenumpress, New York, Vol. 11B, 1992, pp. 1429-1435.
16. Every A. G. and Sachse W., «Sensitivity of inversion algorithms for recovering elastic constants of anisotropic solids from longitudinal wave speed data,» Ultrasonics30, 1992, pp.43-48.
17. Chu Y. C. and Rokhlin S. I., «Stability of determination of composite moduli from velocity data in planes of symmetry for weak and strong anisotropies,» J. Acoust. Soc.Am. 95, 1994, pp. 213-225.

18. Audoin B., Baste S. and Castagnède B., «Estimation de l'intervalle de confiance des constantes d'élasticité identifiées à partir des vitesses de propagation ultrasonores,» C. R. Acad. Sc. Paris 312, série II, 1991, pp. 679-686
19. Hosten B., Hutchins D. and Schindel D., «Measurement of elastic constants in composite materials using air-coupled ultrasonic bulk waves,» J. Acoust. Soc. Am. 99, 1996, pp. 2116-2123.
20. Audoin B. and Bescond C., «Measurement by LASER generated ultrasound of four stiffness coefficients of an anisotropic material at elevated temperatures,» J. Non Dest. Eval. 16, 1997, pp. 91-100.